Analysis of the Complementarity of Two Diagnostic Methods on a PV Generator

Ousmane W. COMPAORE[1,2], Ghaleb HOBLOS[1], Zacharie KOALAGA[2]

{o.compaore@esigelec.fr[1], ghaleb.hoblos@esigelec.fr[2], kzacharie@hotmail.com[3] }

IRSEEM, Esigelec, Unirouen, Normandy University. 76000 Rouen, France[1]

LAME, UFR-SEA, Université Joseph Ki-Zerbo. 03 BP 7021, Ouagadougou, Burkina Faso[2]

Abstract.   The performance of Photovoltaic Generators (PVG) drops over time due to failures compared with its maximum operating point. So, an early fault diagnosis method would make it possible to restore the PVG to good working order. The quality of this diagnostic method lies in several factors but also in the nature of the detection modes. Thanks to the computing capabilities, the analysis databases, and development of efficient algorithms closer to artificial intelligence, we realize that decision support methods are a great success for data science. This article offers an analysis of the complementarity of two diagnostic methods based on the analysis of redundancy relationships and on artificial neural networks. These two methods are supposed to provide a good return on investment for a PVG and set guidelines for diagnostic research.

Keywords: Diagnostic, Analytical Redundancy Relation, Artificial Network Neuron, ROC, AUC, Sensor Fault, System Fault, PVG.

1 Introduction

The photovoltaic market has reached a remarkable level over the last decade, thanks to stimulating factors such as support policies or the reduction of production costs. This has considerably made the rate of return on investment of a photovoltaic installation very attractive. This is how some researchers became interested in finding simple but effective solutions tending to optimize the operation of photovoltaic generators (PVG), subject to anomalies or faults [1].

These faults, which may be intermittent, sudden or incipient, may also disappear or change over time, due to sunlight or environmental constraints in which the generator is supposed to produce. Faults such as yellowing, browning of solar cells, delamination, bubbles, or cracks, which are due to the anti-reflective coating or shading, represent as many indications of faults as anomalies impacting the parameters of the PVG model. Once unsealed early, predictive maintenance actions should be taken to restore the PVG.

Therefore, increasing the reliability and efficiency of PVGs becomes essential through the implementation of proven diagnostic algorithms [1]. Due to the rapid development of computer and

automatic technologies, allied with the requirements of fault detection and diagnosis (FDD) algorithms, which have improved considerably. And thanks to the performance of deep learning (DL) algorithms, smart FDD has become more automated and efficient [2].

PVG, which are also complex [3, 4], have analysis problems that may be related to the nature of their analysis data collection, like the industrial systems treated in [5, 6, 7, 8]. In this article, we try the analysis of the complementarity of two diagnostic methods, one of which is based on the parity space method [9, 10] and the other one on the artificial neural network (ANN) method [11, 12]. The principle of the first method is based on the analysis of redundancy relationships through the generation and structuring of residuals, detection by a statistical test, signature and then isolation of the fault. For artificial neural networks, the main steps are observed through data preprocessing, network design and decision making.

Whatever the method, the preprocessing of the data and the structuring of the residuals encompasses the problem of small samples, which can pose problems for practical applications. There is also the problem of storing and analyzing big data a posteriori. In short, the realization of any diagnostic method depends on the availability but above all on the quality of the data of the process [13]. Practical measurements are usually noisy and infected with errors that sometimes obscure important characteristics of the data and limit the effectiveness of any process monitoring technique [9]. This article also deals with the types of faults diagnosed through its two methods applied to the maximum operating point (MPPT), from the point of view of the methodology and the results obtained.

After having given the position of the problem in section 2, we will present some important elements of the PVG model used in section 3. The outline of each of the diagnostic methods will be done in section 4. The interpretation of the results will be done in section 5. The conclusion that will put an end to this work be taken care of in section 6.

2 Problem statement

This article aims to analyze between two diagnostic methods applied to a PVG, a complex industrial system, which has particularities of non-linearities and defects that can significantly affect its operating performance [1, 2, 13]. The first diagnostic method based on the parity space technique is able to identify sensor faults in a PVG and the second diagnostic method based on the neural network technique is able to identify system faults in the PVG.

In reality, the choice of the FDD is based on the effectiveness of this diagnostic method vis-à-vis an instrumentation based on sensors judiciously placed for the monitoring of the state of health of the PVG, in order to undertake corrective or predictive maintenance actions. The use of sensors, which must be as realistic as possible, is non-invasive and non-intrusive in order to combine electronic efficiency and economy of the on-board instrumentation system.

The major innovation of this work in the application at the MPPT point of the two diagnostic methods, for the structuring of the necessary residuals or for the preprocessing of the data necessary for the analysis of each diagnostic method. The detection and localization of any PVG sensors or systems faults with respect to its considered operating point will also make it possible to judge the relevance of the diagnostic method.

Also, we will judge whether, the two approaches as presented, can be complementary or be combined with a global diagnosis on the PVG.

3   Modeling of PVG

The elementary cell of Bishop's model [3, 4], forms the basis of the model of the PV generator used and illustrated in Figure **1**. Operation is at maximum operating point (MPPT).
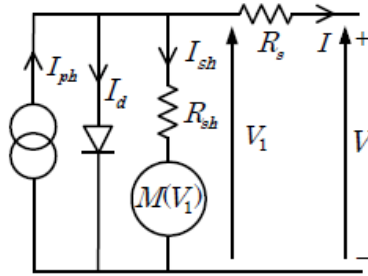
Fig. 1. Bishop model of a PV cell.

The relation (1) gives the output current.

$$I = I_{ph} - I_0 \left[exp((V + R_s I)/(V_t)) - 1 \right] - \left[(V + R_s I)/(R_{sh}) M(V1) \right] \tag{1}$$

with $M(V1) = 1 + k \left(1 - \frac{V + R_s I}{V_b} \right)^{-n}$

Identical N_{cell} cells in series, in the healthy operating mode, to achieve the desired module voltage is protected by a bypass diode. The module thus created is subject to the same temperature and sunshine conditions [3, 4]. The equivalent circuit of the PVG, comprises a number of modules connected in series N_s and a number of branches (chain) in parallel N_p shown in figure **2**; relations (2) to (5) establish the output current and voltage of the created PVG [2, 4].
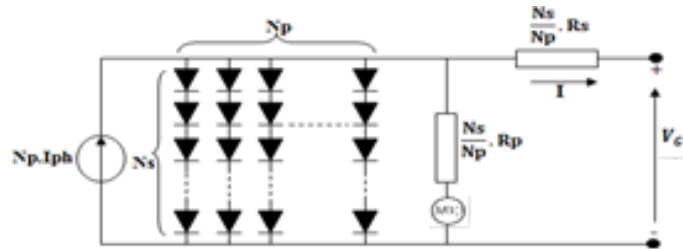
Fig. 2. Modeling of PV generator

Thus, we obtain successively:

- from cell to module through equations

$$\begin{cases} I_c = & I \\ V = & 0.6 \times N_{Cell} \end{cases}$$ (2)

- from module to string by equations

$$\begin{cases} I_{stg} = & I \\ V_{stg} = & N_s * V_m \end{cases}$$ (3)

- from string to field by equations

$$\begin{cases} I_G = & N_p * I_{stg} \\ V_G = & V_{stg} \end{cases}$$ (4)

- finally from the field to the generator by the equations

$$\begin{cases} I_G = & N_p * I \\ V_G = & N_s * N_{Cell} * V \end{cases}$$ (5)

We used sixteen (16) photovoltaic panels, organized in four strings of four modules placed in series, to build the PVG of this study..

The simulation results, with the holy behavior of the PVG through its $I - V$ and $P - V$ characteristics given by Figures **3** and **4**. The two tangent red lines of these two curves allow us to locate the location of the MPPT, for a PVG configured into four strings of four modules in series.
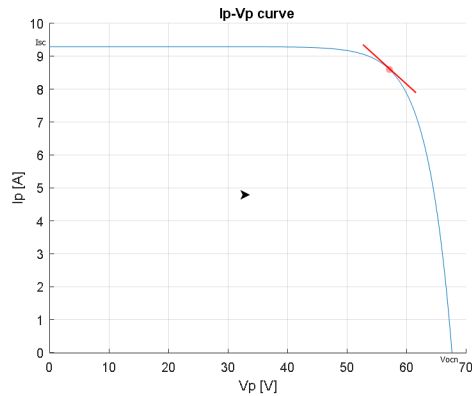
Fig. 3. $I - V$ Characteristic of PVG
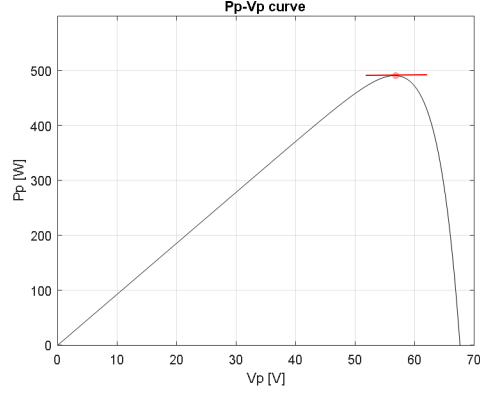
Fig. 4. $P - V$ Characteristic of PVG

4 Diagnosis models

4.1 Approach by Parity Space

The diagnostic method based on the principle of the parity space [3, 7, 13, 14], is based on the analysis of analytical redundancy relations (ARR) whose synoptic is in Figure **5**.

The quantities measured supply the function to calculating the master coefficient a_i and the coefficient of the slope b_i defining the MPPT of generator in equation (6). The structuring of the residuals, then combined in the detection algorithm through the *DCS*, allows the isolation of the sensor faults thanks to the occurrence matrix of Table 1.

$$I_G = a_i * V + b_i \tag{6}$$

with

$$
\begin{cases}
a_i = \left. \dfrac{\partial I\left(I_{\text{stgi}}, V_{\text{stgi}}\right)}{\partial V_{\text{stgi}}} \right|_{\substack{I=Isc \\ V=Voc}} & \text{the coefficient directeur} \\[4ex]
b_i = \left. I_{\text{stgi}} - a_i V_{\text{stgi}} \right|_{\substack{I=Isc \\ V=Voc}} & \text{the coefficient of slopy}
\end{cases}
$$

We obtain the model of the system described by the following equations (7): The form of the measurements given such as:

$$
\begin{cases}
I_G & = I_{stg1} + I_{stg2} + I_{stg3} + I_{stg4} \\
V_G & = V_{stg1} = V_{stg2} = V_{stg3} = V_{stg4} \\
V_{stgi} & = V_{M1stg1} + V_{M2stg1} + V_{M3stg1} + V_{M4stg1}
\end{cases}
\tag{7}
$$
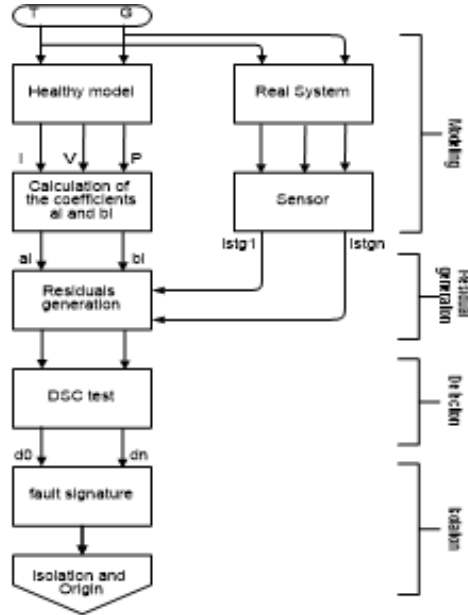
Fig. 5. Diagnosis strategy in an industrial process.

The form of the measurements given such as:

$$\begin{cases} \widehat{I_G} = I_G + \varepsilon_G \\ \widehat{I}_{stg1} = I_{stg1} + \varepsilon_{stg1} \\ \quad \vdots \\ \widehat{I}_{stgp} = I_{stgp} + \varepsilon_{stgp} \\ \widehat{V_G} = V_G + \varepsilon_V \end{cases} \tag{8}$$

where :

- $\widehat{I_G}$ *and* $\widehat{V_G}$ are respectively the current and the voltage measured, using a current sensor and a voltage sensor on the generator;

- I_{stg1} to I_{stgp} and $\varepsilon_{I_{stg1}}$ to $\varepsilon_{I_{stgp}}$ represent respectively the currents measured by current sensors and any noises on the outputs of strings i ;

- ε_V represents any noise on the outputs of the voltage sensor of strings.

All residuals are statistically zero in healthy/nominal case, in normal operation [3], and where the five residuals R_0, R_1, R_2, R_3 *and* R_4, correspond respectively to the five redundancy equations obtained in (9). This observation reflects well the studied sensor fault corresponding to our case

$$\begin{cases} R_0 = \widehat{I}_G - \widehat{I}_{stg1} - \widehat{I}_{stg2} - \widehat{I}_{stg3} - \widehat{I}_{stg4} \\ R_1 = \widehat{I}_{stg1} - a_{i1}\widehat{V}_{stg1} - b_{i1} \\ R_2 = \widehat{I}_{stg2} - a_{i2}\widehat{V}_{stg2} - b_{i2} \\ R_3 = \widehat{I}_{stg3} - a_{i3}\widehat{V}_{stg3} - b_{i3} \\ R_4 = \widehat{I}_{stg4} - a_{i4}\widehat{V}_{stg4} - b_{i4} \end{cases} \tag{9}$$

The different faults structured from the residuals, allows having the occurrence matrix of Table 1 for the isolation and the signature of the expected sensor fault.

Table 1: Occurrence matrix of PVG.

R_i	I_G	V	I_{stg1}	I_{stg2}	I_{stg3}	I_{stg4}
R_0	1	0	1	1	1	1
R_1	0	1	1	0	0	0
R_2	0	1	0	1	0	0
R_3	0	1	0	0	1	0
R_4	0	1	0	0	0	1

The use of the DCS, sum of the likelihood ratio between two probability density functions of two sliding windows, before and after each instant j, is due to its great ability to detect any change in each residual signal, in particular when the change affects the mean and standard deviation [15] at time j. The DCS is defined by equation (12):

$$DCS(t) = \sum_{j=t_{p-1}}^{t} \frac{1}{2}[\log\frac{(\gamma_a^2)^j}{(\gamma_b^2)^j} + \frac{(\varepsilon_a^2)^j}{(\gamma_a^2)^j} - \frac{(\varepsilon_b^2)^j}{(\gamma_b^2)^j}] = \sum_{j=t_{p-1}}^{t} S_j, \ t \geq t_{p-1} \tag{10}$$

with s_j the logarithm of the likelihood ratio, with $\theta_a^j = (\gamma_a^2, a_1^a, ..., a_p^a)^j$, the first window estimate; γ_a^2, the scalar random variable variance θ_a and ε_a the mean and $\theta_b^j = (\gamma_b^2, a_1^b, ..., a_p^b)^j$, the second window estimate; γ_b^2, the scalar random variable variance θ_b and ε_b the mean.

The detection function used to estimate the instant of change is given by:

$$g(t) = \max_{t_{p-1} \leq j \leq t}[DCS(j) - DCS(t)] \tag{11}$$

The stop instant can therefore defined as:

$$t_p = \inf\{n > t_{p-1} : g(n) > h\} \tag{12}$$

With h the detection threshold to be defined.

The results of the simulation of this method summarized in the two Figures **6** and **7**, with the treatment of the residuals, $R_0 and R_3$. They show respectively the DCS, $g(t)$ and detection functions. The treatment of residuals $R_1, R_2 and R_4$ has not been shown. The amplitude 2A fault, having entered

string 3, affects the R_0 and R_3 residuals of Figures **6** and **7**. The juxtaposition of all the detection functions in Figure **8** makes it possible to isolate the sensor fault of string 3, according to the occurrence matrix of Table 1.

Failures occurring at any time, the operation of the PVG depends on particular cases, resulting from the elimination of all assumptions. Therefore a certain failure of the sensors is necessary for the validation of the data used in this diagnostic method. This guarantees the reliability and operational safety of the system, but also guarantees a high return on investment.
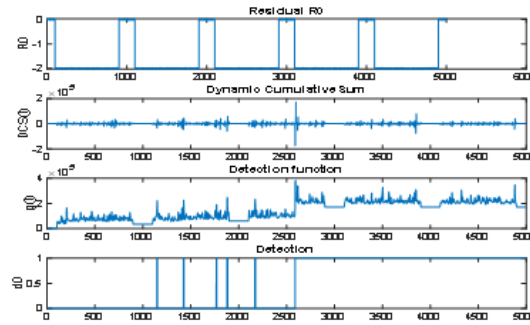
Fig. 6. Residual R_0.
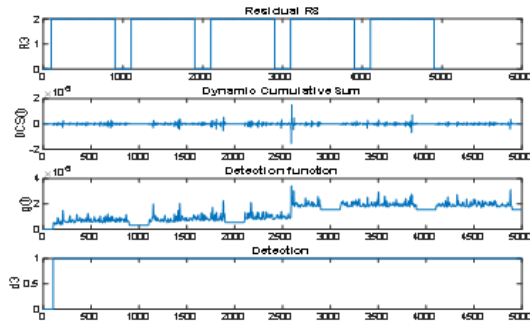
Fig. 7. Residual R_3.

4.2   Approach by Artificial Neuronal Network (ANN)

If the previous diagnostic method warns of sensor faults, it is a good idea to use this other method to consider the special case of PVG system faults.

First, remember that the power loss of a PVG depends on several factors related to the characteristics of the materials, the protective components or the environmental or meteorological conditions. These operating anomalies prove to be closely linked to the known parameters of the PVG, such
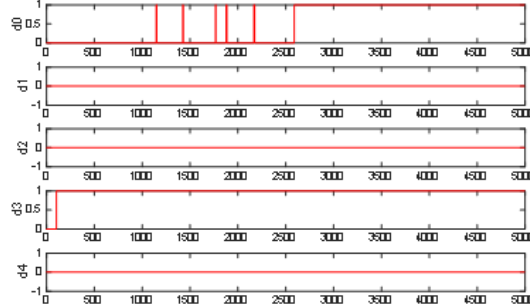
Fig. 8. Superposition of 5 detection fonction.

as $R_s, R_{sh}, N_{cell}, I_{ph}, T\ or\ G$, used during the simulation under Simulink. The resulting failure mode which remains a special case of operation of a photovoltaic generator in healthy mode, linked to one of the parameters mentioned above. Therefore this refers to a faulty behavior of the system. We are also going to try the automatic learning approach for detecting system faults through, the use of artificial neural networks on the PVG [10, 12, 14].
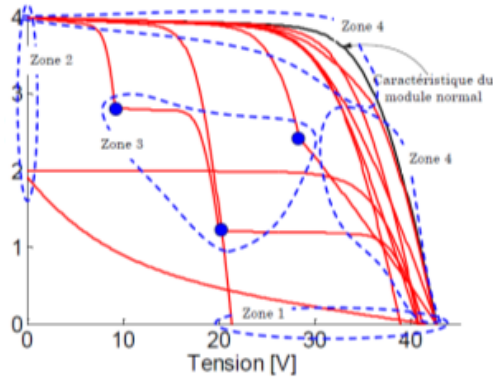
Fig. 9. $I-V$ characteristic in healthy (black)/failure mode (red).

Second, we have in Figure **9** of the I-V characteristic of the PVG, according to [16], a form of classification of the faults into five zones, to understand its behavior.

- The first obvious fault, the loss of power produced, suggests the presence of a fault. Which is not obvious, because some faults do not cause any loss of power. For example when the anti-return diode is disconnected.

- The second fault in "*Zone*1" is a voltage fault in zone 1 in Figure **9**. Such as a torn module (R_s, R_{sh}) or short cicuity, or a rise in temperature (T).
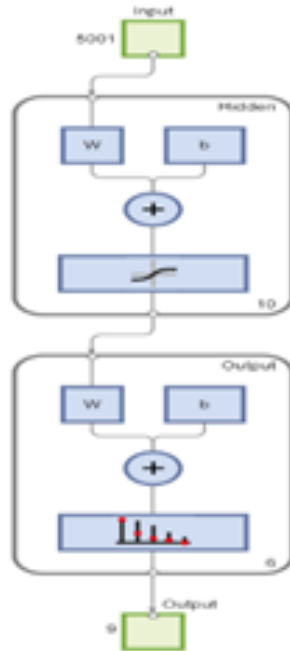
Fig. 10. ANN structure.

- The third fault in "*Zone*2" is a current fault in zone 2 in Figure **9**. Such as the loss of a string module (R_s, R_{sh}) or a bad sun (G).

- The fourth fault in "*Zone*3" refers to the abrupt deviation of the $I - V$ characteristic with the emergence of one or more inflection points located in Zone 3 of the Figure **??**. This is the case of the loss of a set of modules in a string (N_{cell}, R_s, R_{sh}).

- The fifth fault in "*Zone*4" refers to the deviation of the slope of the faulty $I - V$ characteristic from that in healthy operation [16]. It is no gap if the voltage and current drop profile are constant along the $I - V$ curve in black. Otherwise, attention will be focused on :

  - the voltage drop profile in the vertical zone 4 of Figure **9**, corresponding to an increase in the serie resistance (R_s) synonymous with shading;

  - to the profile of the current drop in the horizontal zone 4 of Figure **9**, corresponding to a reduction in the shunt resistance R_{sh}.

Knowledge of PVG behavior modes can then codified in the simplified signature table given in Table 2 [16]. It will also serve as an output matrix. The three-bit binary coding will simply by used for interpretation during the simulation.

Table 2: Signature of faults.

Code	P	V	I	Default Designation
000	0	0	0	Healthy mode
001	0	0	1	Mismatch type shade or sunshine
010	0	1	0	Short-circuited or reverse module
011	0	1	1	Mismatch type partial shade, or dirt
100	1	0	0	Bypass or Mismatch type R_{sh} or R_s
101	1	0	1	Bypass or Mismatch type R_s or R_{sh}
110	1	1	0	Mismatch type R_s
111	1	1	1	Fault nature is Unknown

Third, we recall that ANN consists of an input layer, an output layer with hidden layers. The neurons and their arc weights represent the basic components of the ANNs, while the weight of the input-output functions participates as a criterion for evaluating the performance of the ANN [17]. The main difference between the two types of architectures lies in the feedback between the network during the back-propagation stage, which is present when using a recursive architecture with good prediction. In this article, the Levenberg–Marquardt back propagation (LMBP) algorithm is put forward for the multilayer formation of ANN. It is an algorithm that has been widely used in learning feedforward multilayer neural networks. Its supervised learning technique is based on the Gradient Descent method, which consists in minimizing the error of the network by descending the slope of the error curve [8, 11]. The main advantage of the back propagation algorithm is that it is easy and efficient to implement for an ANN in order to improve its efficiency by updating the solution at each iteration [17]. The use of the Levenberg-Marquardt algorithm aims to find an optimal solution to Gradient Descent combined with the Gauss-Newton [3] algorithm. Moreover, this learning Levenberg-Marquardt algorithm allows performing classification tasks.

Fourth, the ANN proposed in Figure **10**, built with inputs from the power, voltage and current measurements of the PVG, i.e. $3 * 5001$, 10 hidden layers arbitrarily set by Matlab software and $3 * 9$ outputs contained in Table 1. The data ANN training uses the data contained in the input matrix, organized as follows:

- 70% will be used for training;

- 15% will be used to validate the generalized network and stop the formation of the adjustment;

- the remaining 15% will be used in an independent test of network generalization.

The results of the simulation of this method of the learning algorithm performed on the 1000 epochs. Figure **11** shows the descent of the learning error. The descent of the gradient, not presented here is quick good arround 0.0072131 at epoch 1000. The plot of the ROC curve, i.e. the ratio of the rate of true positives (*sensitivity*) compared to the rate of false positives ($1 - specificity$) when the threshold varies, is illustrated in Figure **12**, attests to the good performance of the ANN for diagnosis of our PVG. The network is therefore configured to assimilate the behavior of the PVG well, as it

has dots in the upper left corner, with a sensitivity of 100% and a specificity of 100% for all tests. The good performance on the training set combined with the poor performance on the test set, is synonymous with an overfitting of the model because the curve will pass through the first bisector. A reduction in the number of neurons makes it possible to reduce this overfitting.

Finally, to improve the performance of the network configured in this way, you can either : retrain the network or increase the number of hidden neurons, and using a larger training dataset, which turns out to be the eternal problem of ANN-based solutions.
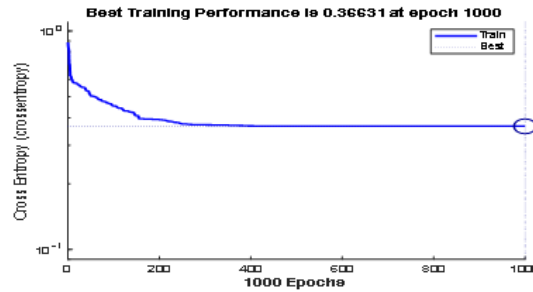
Fig. 11. The training performance.
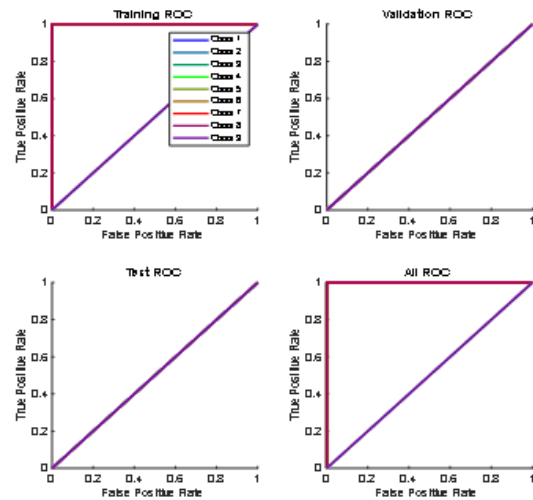
Fig. 12. ROC curve.

For this application, we operate a double variation of the temperature and the level of sunshine in order to collect the input data. The compilations thanks to the output matrix, gives the signature of the system faults, in connection with one of the parameters of the system, thanks to Table 2.

System faults make it possible to undertake maintenance actions close to the reality of the system, especially since code faults, $001, 011, 100, 101$ *and* 110 all refer to faults of the mismatch type linked either to shading or to an illumination of PVG.

5 Interpretations of results

From the results obtained, we can make the following analysis :

- The common point of these two methods lies in the collection of data. It is done using simple, economical and non-invasive instrumentation in sensors, for real-time acquisition, of data such as string currents, voltage, current and power of PVG.

- For the first method, the generation of residuals is required through the calculation of error signals between the outputs of the faulty system and those of the process obtained by measurements.

- For the detection function through the DCS, setting a threshold for each fault is necessary, but an analysis of the performance is necessary through the ROC curve in order to find the ideal detection threshold, to avoid false detection.

- On the other hand, the establishment of detection threshold in the parity space method is difficult to harmonize from one fault to another, as this can leads to false alarms and poor fault detection.

- The detection of sensor faults, highly localizing, thanks to the occurrence matrix, makes it possible to rule out any shortcoming of the measuring instruments if necessary, but remains limiting as regards faults relating to the physical system.

- In the case of the deep learning technique based on the ANN, it is based on a database to classify the faults on the nine classes arbitrarily chosen, thanks to the coding of the output matrix of Table 3. Our network built, thanks to the real input data P, V and I, resulting from the measurements of the PVG. The ten hidden layers (arbitrarily set by Matlab) of the algorithm improve the learning performance of our diagnostic method.

- Learning by ANN is quite simple and allows us to classify system faults through training errors and weak learning. The nature of the faults diagnosed generally related to one of the parameters of the system model. The use of the LM algorithm makes it possible to find an optimal solution to the gradient descent quite quickly.

- Finally, we can say that the quality of one or another diagnostic method depends on the quality of the available process data. In addition, it will be necessary to take into account the high level of noise influencing the quality of the measurements from the instrumentation and real-time acquisition system, and therefore the quality of the data used.

6 Conclusion

The method of the parity space, which principle is based on the technique of the analysis of the relations of redundancy, applied to the MPPT and is quite effective according to our results. This technique undoubtedly makes it possible to rule out all types of sensor faults, which can be located by our occurrence matrix. This method also suffers from the fixing of the detection threshold for each defect. By providing more equation related to the knowledge of the system, this technique could be able to diagnose faults close to the system.

The same diagnostic problem has been applied to the PVG, thanks to the Deep learning technique based on RNA algorithms (simple and easy) once well configured, will represent a good diagnostic tool for the PVG. Data pre-processing, network design and decision support is done taking into account the complexity and non-linear dynamics of this industrial process.

The two approaches do not target the same type of faults. Because the parity space is aimed at system sensor faults, while the ANN is aimed at system faults. We can therefore consider deepening the actions in order to make them complementary or to combine their principle of action, in view of a global diagnosis on the PVG going in the direction of the improvement of one or the other method.

The Parity space can improve but on condition of having more physical relationships, close to the real behavior of the model. Whereas the ANN is more sensitive in terms of locating faults in relation to the very part of the system in default, which is related to one of its parameters.

Detecting and diagnosing faults are an effective solution for making PVG efficient and reliable, but above all for guaranteeing a good return on investment.

References

[1] Compaoré, O. W. Hoblos, G. and Koalaga, Z. Analysis of the impact of faults in a photovoltaic generator. International Conference on Innovation and Intelligence for Informatics, Computing, and Technologies (3ICT), Bahrein, 2021, pp. 68-73, doi: 10.1109/3ICT53449.2021.9581575. (2021).

[2] Basnet B, Chun H, and Bang J. An intelligent fault detection model for fault detection in photovoltaic systems. J. Sensors, vol. 2020, pp. 1-11, Jun. 2020.

[3] Ait-Izem T, Harkat M.-F, Djeghaba M, and Kratz F. Sensor fault detection based on principal component analysis for interval-valued data. Qual. Eng., vol. 30, no. 4, pp. 1-13, 2017.

[4] Bishop, J. Computer Simulation of the Effects of Electrical Mismatches in Photovoltaic Cell Interconnection Circuits. Solar Cells, 25:73-89 (1988).

[5] Zhang Z, Li X, Wen L, Gao L, and Gao Y. Fault diagnosis using unsupervised transfer learning based on adversarial network in Proc. IEEE 15th Int. Conf. Autom. Sci. Eng. Aug. 2019, pp. 305-310.

[6] Shao H, Jiang H, Zhang H, and Liang T. Electric locomotive bearing fault diagnosis using a novel convolutional deep belief network. IEEE Trans. Ind. Electron., vol. 65, no. 3, pp. 2727-2736, 2017.

[7] Ebha K, Anamika Y, Thoke A. S, Abhinav J, and Subhojit G. Detection and Classification of Faults on Six Phase Transmission Line Using ANN. 2nd International Conference on Computer and Communication Technology, 'ICCCT', Allahabad, India. 5-17 September, 2011.

[8] Tao J, Liu Y, and Yang D. Bearing fault diagnosis based on deep belief network and multisensor information fusion. Shock Vib., vol. 2016, pp. 1-9, Aug. 2016.

[9] Gao S, Shi L, and Zhang Z. A Peak-Over-Threshold Search Method for Global Optimization', Automatica. Vol. 89, pp. 83-91, 2018.

[10] Zortea M, Flores E. S, and Scharcanski J. A Simple Weighted Thresholding Method for the Segmentation of Pigmented Skin Lesions in Macroscopic Images. Pattern Recognition, Vol. 64, pp. 92-104, 2017.

[11] Zhao B, Lu H, Chen S, Liu J, and Wu D. Convolutional neural networks for time series classification. J. Syst. Eng. Electron., vol. 28, no. 1, pp. 162-169, Feb. 2017.

[12] Sun G, Liang L, Chen T, Xiao F, and Lang F. Network traffic classification based on transfer learning. Comput. Elect. Eng., vol. 69, pp. 920-927, Jul. 2018.

[13] Kang M, Islam M. R, Kim J, Kim J. M, and Pecht M. A hybrid feature selection scheme for reducing diagnostic performance deterioration caused by outliers in data-driven diagnostics. IEEE Trans. Ind. Electron.,vol. 63, no. 5, pp. 3299-3310, May 2016.

[14] X. Huang, X. Zhang, Y. Xiong, H. Liu, and Y. Zhang, "A novel intelligent fault diagnosis approach for early cracks of turbine blades via improved deep belief network using three-dimensional blade tip clearance," IEEE Access, vol. 9, pp. 13039-13051, 2021.

[15] El Falou, W. Duchêne, J. Khalil, M. A. AR-based method for change detection using dynamic cumulative sum. Proceedings of the 7th IEEE International Conference on Electronics, Circuits and Systems ICECS 2000, Vol. 1, Jounieh, Lebanon, pp. 157-160.

[16] Compaoré, O. W. Hoblos, G. and Koalaga, Z. Artificial Neural Network based fault diagnosis in an isolated photovoltaic generator. In 4th Conf EAI. JRI 2021. DOI: 10.4108/eai.11-11-2021.2317977.

[17] Karmacharya I, and Ramakrishna G. Fault Location in Ungrounded Photovoltaic System Using Wavelets and ANN. IEEE Transactions on Power Delivery, Vol. 33, N°2, pp. 549 - 559, 2017.